ACS APPLIED MATERIALS & INTERFACES

Research Article

www.acsami.org

Synthesis of Disulfide-Cross-Linked Polypeptide Nanogel Conjugated with a Near-Infrared Fluorescence Probe for Direct Imaging of Reduction-Induced Drug Release

Tao Xing, Chengqiong Mao, Bin Lai, and Lifeng Yan*

Hefei National Laboratory for Physical Sciences at the Microscale and Department of Chemical Physics, CAS Key Laboratory of Soft Matter Chemistry, University of Science and Technology of China (USTC), Hefei, 230026, People's Republic of China

Supporting Information

ABSTRACT: Reduction-sensitive polymeric nanocarrier with near-infrared fluorescence probe has been prepared. Disulfide-cross-linked polypeptide nanogel with near-infrared fluorescence property (NIRF nanogel) was first synthesized, then the anticancer drug doxorubicin was encapsulated into polypeptide core of the NIRF nanogel to prepare a drug carrier with near-infrared fluorescence (NIRF prodrug). In vitro drug release study of the NIRF prodrug revealed an accelerated release behavior in the presence of 10 mM glutathione (GSH). Cellular uptake studies of both the NIRF nanogel and NIRF prodrug showed that they could enter cell via endocytosis. With the aid of NIRF labeling, direct imaging of the drug release from NIRF nanogel was accomplished, and drug molecules released subsequently migrated into nucleus while the NIRF nanogel still remained in cytoplasm. In vivo distribution of the NIRF nanogel and NIRF prodrug on tumor-bearing nude mice shows that both of them accumulated at tumor place at 24 h after tail veil injection via enhanced permeability and retention (EPR) effect. The NIRF prodrug prepared here has the potential application for the theranosis of cancer.

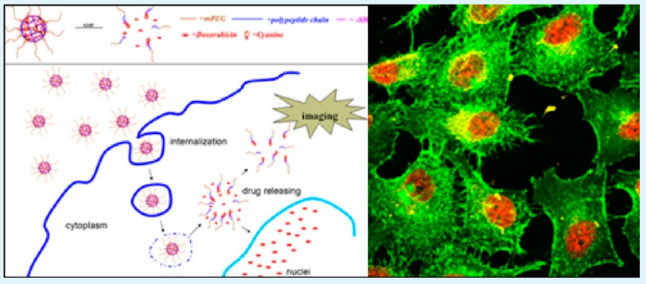

KEYWORDS: *polypeptide, nanogel, disulfide linkage, near-infrared fluorescence, theranosis, drug delivery*

INTRODUCTION

Polymeric nanoparticles are potential drug delivery systems for intravenous drug transportation, and they hold great hope in future clinical use.[1−4] Embedding drugs into nanoparticles not only effectively suppresses its interaction with blood component but also reduces its nonspecific accumulation in biological system, which is usually assumed to cause pronounced toxicity. Besides, versatile synthetic methods also afford the possibility to prepare nanocarriers with other desired properties, such as targeting and imaging ability. Micelle systems self-assembled from linear amphiphilic polymer are mostly used as drug carriers,[5−7] even though these systems are stable only above their critical micelle concentration (CMC). Cross-linked polymeric systems such as core or shell cross-linked polymers[8−10] and branched polymer[11−13] may be more suitable, but they only work well if the cross-linked state could be disassembled after the drug carrier reaches the target. Smart carrier systems,[14−16] which could release the loaded cargo under certain environmental stimulus, seem to be much more promising candidates for drug delivery. Various environmental factors such as pH[8,15] and reduction[17] have been utilized as a stimulus to trigger the release of loaded drugs. The design rationale of reduction-sensitive nanocarriers lies in the fact that GSH, which acts as a reducing agent to reduce disulfide to free thiol, has an inside cell concentration three orders higher than that outside the cell.[18] Destabilization of disulfide-cross-linked materials under this condition leads to a triggered release of the loaded cargo.

Bioimaging is a useful method of extracting desired information from a living body, which is helpful for diagnostics and treatment of cancer. By delicate designation, bioimaging systems with different functionalities that could locate tissues of interest can be obtained. A drug delivery system with bioimaging ability also affords the possibility of precise location of the drug carrier, providing useful information both for the diagnosis of disease and its subsequent treatment. Incorporating various bioimaging agents such as quantum dots,[19,20] iron oxide,[21] radionuclide agents,[22,23] and organic dyes[24−27] into nanocarrier has been performed for these purposes. Among the various imaging methods developed, optical imaging is widely utilized, because of its noninvasive nature and posing less safety issues. Imaging with visible light is a prevalent method for intravital microscopy, but it can be problematic when live body imaging is involved, because of the potential interference from hemoglobin and endogenous molecules. Strong absorption from hemoglobin can be detected at wavelengths lower than

Received: August 9, 2012
Accepted: September 14, 2012
Published: September 14, 2012

   dx.doi.org/10.1021/am301600u | ACS Appl. Mater. Interfaces 2012, 4, 5662−5672

Scheme 1. Illustration of the NIRF Prodrug Endocytosis and Its Subsequent Diassembly and Drug Release Triggered by GSH

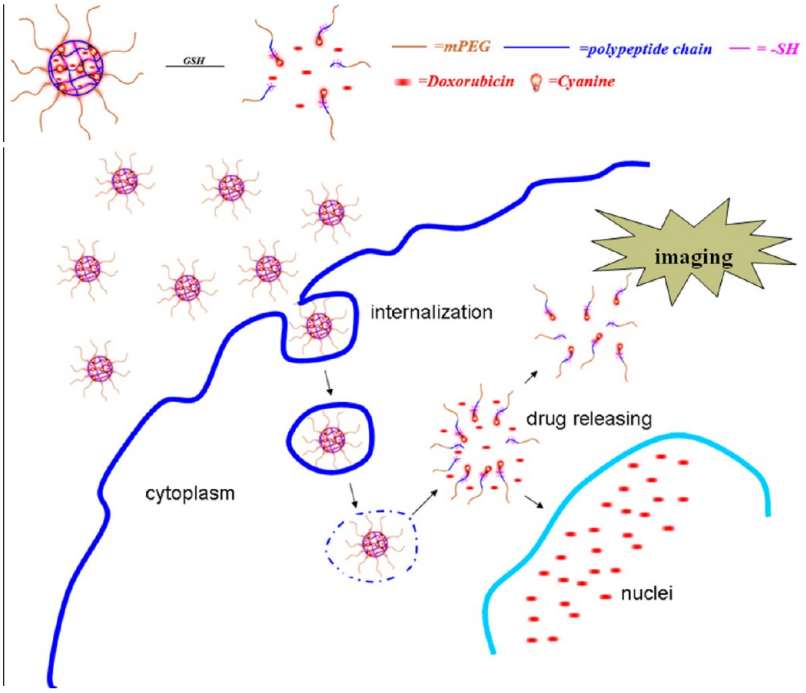

600 nm and significant background fluorescence from endogenous biomolecules can be detected up to wavelengths of 680 nm.[28] Imaging in the near-infrared region (>700 nm), on the other hand, has been widely used for live body imaging, because it works in a wavelength range where body tissue has the least interference.

Cyanine dye is the most widely used long-wavelength imaging agent with commercial availability and FDA approval for clinical use. Despite its excellent optical property for bioimaging, its instability greatly limits its use as bioimaging agents. Inserting a rigid cyclohexenyl ring into the polymethine chain was found to not only increase the stability of the original dye and but also generates another site for further functionalization,[29] while nucleophilic substitution of the Cl atom on the cyclohexenyl ring with amine was found to yield aminocyanine with large stock shifts and stronger fluorescence.[30] Physical encapsulation or chemical conjugation cyanine dye into the polymeric nanocarriers provides another method to improve the dye stability, because it prevents its interaction with either solvent or other dye molecules. Compared with physical encapsulation, chemical conjugation of the dye molecules to the nanocarrier may be more suitable in that it prevents the dye from leakage during blood circulation, thus prolonging the fluorescent time of the system.

Polypeptide material is one type of biodegradable material that has been widely used as a biomaterial during recent years.[31,32] Compared with traditional solid-phase synthesis, ring-opening polymerization of activated amino acid monomer *N*-carboxy-anhydrides (NCA) provides an effective and facile method for the preparation of high-molecular-weight polypeptide. Polymerics system composed of poly amino acid building blocks such as polylysine[33] and poly-L-aspartic acid[34] have been widely employed for the preparation of gene and drug delivery systems.

Here, we report the synthesis of a novel reduction-sensitive drug delivery system with near-infrared fluorescence, and try to image directly the drug release process upon endocytosis. A schematic illustration of the NIRF prodrug internalization and its subsequent drug release is shown in Scheme 1. Scheme 2 shows the synthetic route of the NIRF polypeptide nanogel. Cyanine dye (**3**) was synthesized by condensation of quatemary ammonium salt (**1**) and bisaldehyde (**2**) in a mixture solvent of butanol and benzene. Dye **3** was then transformed to aminocyanine (**4**) by reacting with 1 equiv of aminocaproic acid. Parent nanogel (**8**) was synthesized by a one-step ring-opening copolymerization of nepsilon-carbobenzoxy-L-lysine NCA (LLys NCA) (**6**) and L-cystine-NCA (**7**) with amino-terminated poly(ethylene glycol) methyl ether (mPEG). NIRF nanogel (**9**) was prepared by a peptide coupling reaction between an activated form of aminocyanine (**4**) and the parent nanogel (**8**). Anticancer drug was then encapsulated into the above NIRF nanogel to prepare NIRF prodrug, which shows reduction promoting drug release behavior in the presence of 10 mM GSH. Because of the near-infrared fluorescence property of the NIRF prodrug, the drug delivery process could be conveniently monitored in vivo. A whole-body imaging experiment on nude mice shows that both of the NIRF nanogel and NIRF prodrug could successfully accumulate in the tumor's place within 24 h via ERP mechanism. Cellular uptake studies of NIRF nanogel and NIRF prodrug show that both of the two materials could enter the cell via endocytosis.

RESULTS AND DISCUSSION

The cyanine dye (**3**) was prepared according to a literature reported method,[35] via condensation of quatemary ammonium salt **1** with bisaldehyde **2** in a mixture of benzene and *n*-butanol. It is noteworthy that the side carboxyl group of quatemary ammonium was also esterified during this process, thus leading to the formation of *n*-butyl ester protected cyanine dye. Various nucleophilic reagents, such as thiol, alcohol, and amine, have been used to replace the Cl atom on the central ring to prepare a functionalized cyanine dye, while only substitution of the Cl

dx.doi.org/10.1021/am301600u | ACS Appl. Mater. Interfaces 2012, 4, 5662−5672

Scheme 2. Synthesis of Cyanine-OSu 5 and NIRF Nanogel

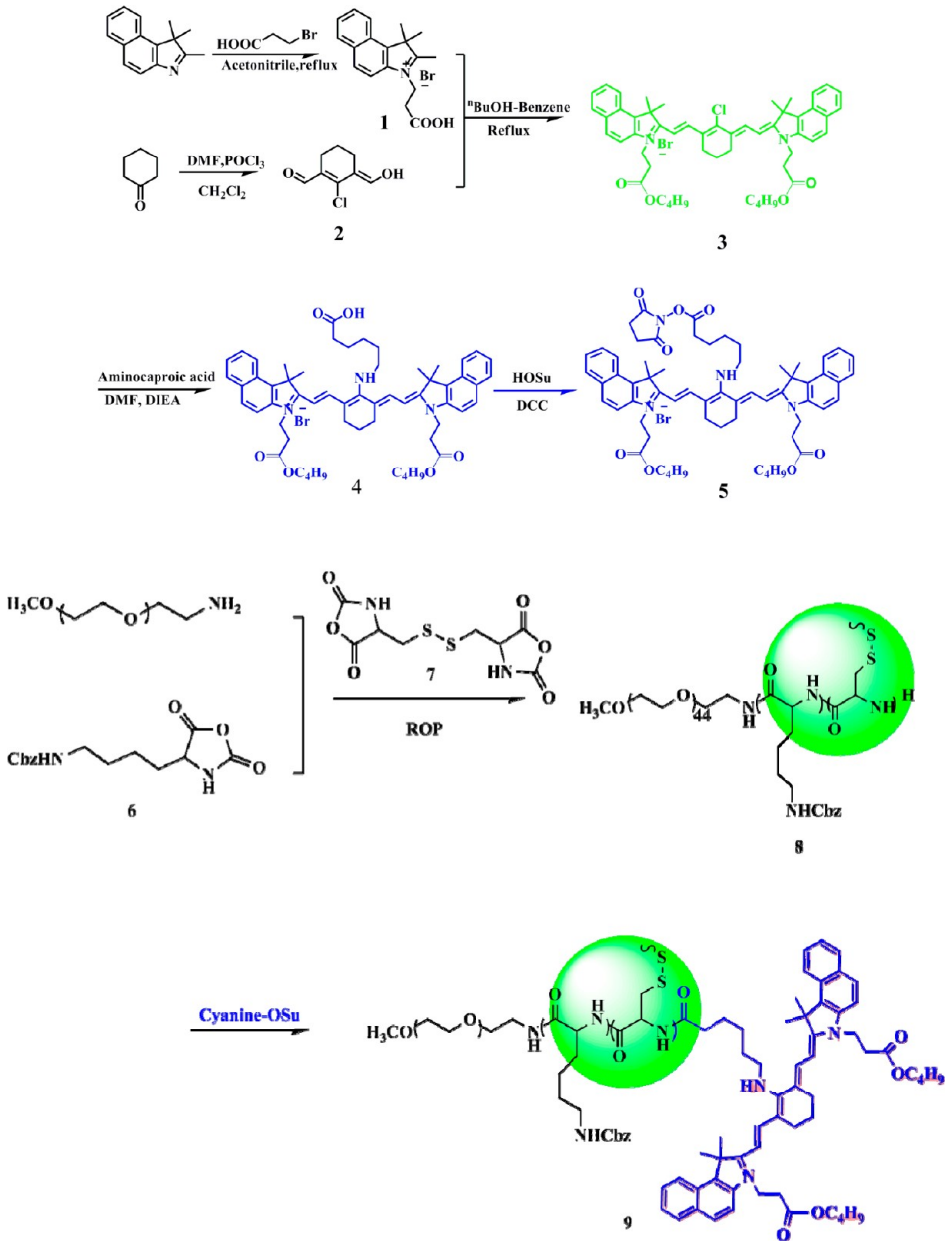

atom with amine was found to simultaneously improve the dye's stability and optical properties.[30] The resulted aminocyanine has a large stock shift, which makes it especially intriguing for bioimaging, because self-quenching was minimized under this condition. So cyanine **3** was then converted to aminocyanine **4** by a nucleophilic substitution with aminocaproic acid. Mass spectra of cyanine **3** and aminocyanine **4** are shown in Figures S1 and S2 in the Supporting Information; in both cases, the related molecular cation peak $[M-Br^-]^+$ could be observed. Intermediate cyanine-OSu (**5**) was prepared via the reaction of **4** with HOSu in the presence of 1.3 equiv of DCC as a dehydrating agent. Because of the moisture-sensitive nature of **5**, it was used directly for nanogel labeling without purification.

Ring-opening polymerization of NCA provides a facile and economical way to prepare polypeptides with high molecular weight. The final polypeptide can be either a branched[36−38] or linear[39] structure, depending on the starting monomers and initiators utilized. NCAs with various side groups also afford the possibility of preparing polymers with various functional side groups. Here, L-cystine-NCA was chosen for incorporation because the polymerization of this difunctional monomer would result in the formation of a core-cross-linked star (CCS) polymer with a disulfide-cross-linked polypeptide core.[40] The synthetic procedures are shown in Scheme 2. Polymerization was carried out at 0 °C for 3 days, followed by heating to 45 °C for one day to drive the reaction to completion. Evolution of the polymerization was monitored by analyzing the polymerization solution with FT-IR spectra. As shown in Figure 1a, after stirring at 0 °C for 3 days, the absorption corresponding to the anhydride moiety could still be observed at 1780 and 1850 cm^{-1}, while the absorption corresponding to the anhydride bands completely disappeared after stirring for another day at 45 °C (96 h), indicating the completion of the polymerization. ^1H NMR result of the nanogel was shown in Figure 1b. Signals corresponding to the mPEG moiety could be observed at 3.50

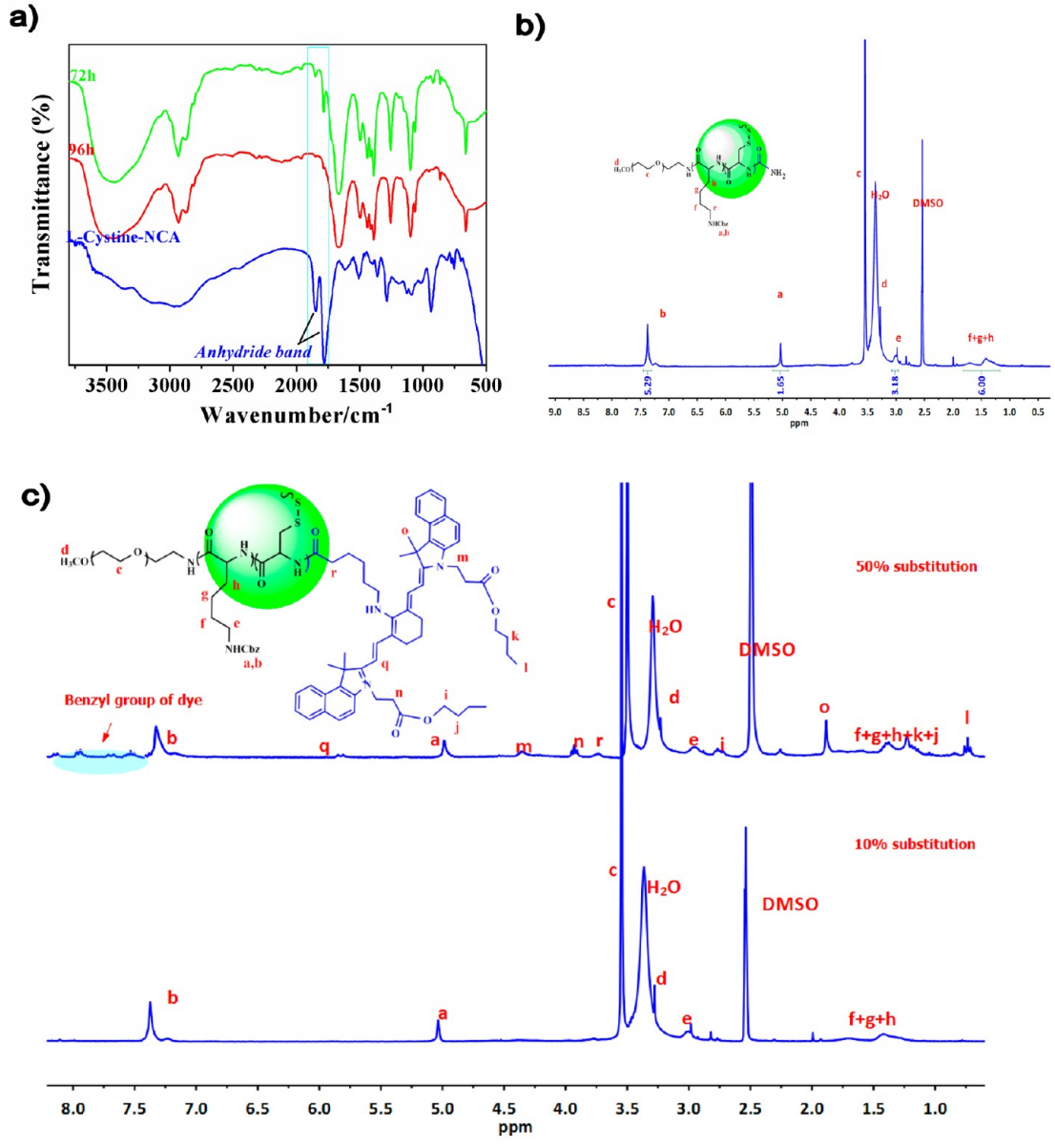

13

Figure 1. (a) FT-IR spectra of the polymerization solution at various reaction stages. FT-IR spectrum of L-cystine-NCA was used as a reference; (b) ^{1}H NMR spectrum of parent nanogel in DMSO-d_6; (c) ^{1}H NMR spectrum of NIRF nanogel at different degree of dye substitution in DMSO-d_6.

ppm ($-C\underline{H}_2CH_2O-$) and 3.22 ppm ($-C\underline{H}_3O$), and chemical shifts at 5.06 ppm ($C_6H_5-C\underline{H}_2-$) and 7.34 ppm ($C_6\underline{H}_5-CH_2-$) could be attributed to the carbobenzyl ester group of LLys-NCA. Signals appearing at 2.80 ppm ($Cbz-C\underline{H}_2-$) and 1.30 ppm ($Cbz-NH-(C\underline{H}_2)_3-$) are corresponding to the methane group of side group of LLys-NCA. Methylene group adjacent to sulfide could not be observed in ^{1}H NMR spectrum, because of its overlap with H_2O or signal suppression resulting from the cross-linked nature of the core.[41]

Various synthetic methods such as copper-catalyzed azide alkyne cycloaddtation (CuAAc),[42,43] strain promoted azide alkyne cycloaddition (SPAAc),[42] peptide coupling,[26,44,45] and direct radical nucleophilic substitution[42] have been utilized for labeling macromolecules with cyanine dye. Among the above methods developed, CuAAc and SPAAc methods are characterized by high conjugation efficiency but limited to the requirement of both azide- and alkyne-group-containing molecules which usually require multiple steps to prepare. Besides, the copper residue after conjugation, which is usually difficult to remove, also limits its use for biomolecules labeling. Peptide coupling method between an activated carboxyl group and an amine group, on the other hand, could be performed under mild reaction condition and thus was routinely utilized for peptide labeling. Here, this facile method was adopted because of the retention of primary amine groups after ring-opening polymerization of NCA, and the labeling was thus straightforward without additional treatments. For NIRF materials preparation, hydrophilic cyanines that usually contain mutil-sulfonic acid groups were employed,[26,27,42] and the purification of those high polar molecules was usually very difficult while the yields remain low. Here, a hydrophobic cyanine dye (**4**) was utilized, because hydrophobic dyes are much easier to obtain with satisfied yields via normal phase column chromatography. Labeling with hydrophobic cyanine

molecules may be a more economical and promising method for future tumor imaging.

The ^{1}H NMR spectrum of NIRF nanogel (**9**) is shown in Figure 1c. Dye signals could only be discerned when a higher percentage (25% and 50%) of the terminated primary amine was coupled with aminocyanine. At a coupling rate of 10%, the spectrum is poorly resolved and only shows signals of nanogel moiety. This may be because the fixation of dye molecules onto the nanogel skeleton reduces mobility of dye molecules and leads to the suppression of their signal.[46,47]

Chemical composition of both the parent nanogel (**8**) and NIRF nanogel (**9**) (10% dye substitution) were determined by elemental analysis, as shown in Table 1. The elemental content, calculated based on feed ratio, was listed for reference. In both cases, the elemental composition was quite close to the calculated value, indicating the formation of the target nanogel.

Table 1. Elemental Composition of the Parent Nanogel and NIRF Nanogel, as Determined by Elemental Analysis

	composition (wt %)			
sample	N	C	H	S
parent nanogel	6.64[a]	52.18	7.27	7.52
	6.38[b]	51.01	7.22	7.69
NIRF nanogel	6.31[a]	51.58	7.42	7.47
	6.14[b]	50.14	7.21	7.36

[a]Elemental content determined by calculation based on feed ratio. [b]Elemental content determined from results measured using an elemental analyzer.

Figure 2 shows the absorption and emission spectra of both the parent nanogel **8** and the NIRF nanogel. Compared with its parent nanogel solution, the NIRF nanogel solution was blue in appearance and has a strong absorption and emission at 650 and 730 nm, with a large stock shifts of 80 nm. Cyanine dye is known to form aggregate of H or J shape, in both aqueous and organic solution.[48] Here, the NIRF nanogel solution only shows a single absorption peak at 650 nm, indicating no aggregation of the dye molecules in this case. This may because the conjugation of dye molecules to the nanogel skeleton restricts their mobility, thus eliminating their tendency to aggregate. Quantum yields of the NIRF nanogel with different degrees of dye substitution are shown in Table 2. Incorporating more dye molecules into the parent nanogel **8** leads to a decrease in quantum yield, which may be attributed to the self-quenching of dye molecules at a higher dye coupling rate.

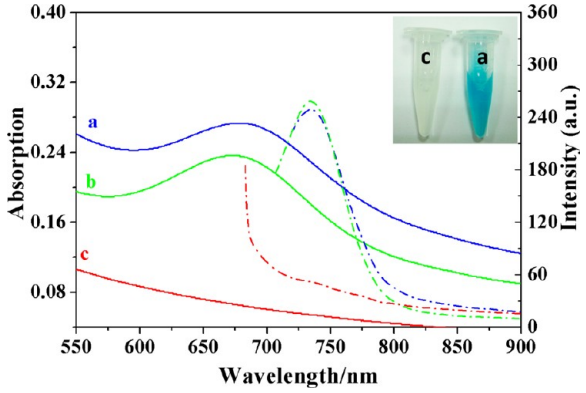

Figure 2. Absorption (solid line) and emission spectra (dashed line) of the NIRF nanogel (0.1 mg/mL) in H_2O (spectrum a) and PBS (spectrum b). Absorption and emission of the parent nanogel aqueous solution (spectrum c) was used as a reference. All emission spectra were excited at 670 nm. Inset shows a digital camera image of parent nanogel (c) and NIRF nanogel (a) aqueous solution.

Table 2. Quantum Yields of NIRF Nanogel at Different Degrees of Dye Substitution

	Quantum Yields of NIRF Nanogel		
	10% substitution	25% substitution	50% substitution
Φ_F	0.163	0.030	0.019

Size and size distribution of both the parent nanogel and NIRF nanogel solution were studied by dynamic light scattering (DLS), and the results are shown in Figures 3a and 3b, respectively. TEM images of the two nanogels were also presented for reference. For theparent nanogel, the mean diameter determined by DLS measurement is 275 nm, which is slightly larger than the size given by TEM measurement (~250 nm), and this may due to the shrinkage of the nanogel after solvent evaporation during sample preparation. The mean diameter of the NIRF nanogel solution measured by DLS was 232 nm, while in the TEM image, the diameter was ~200 nm.

The drug was loaded into the NIRF nanogel by mixing the DMF solutions of drug and polymer at room temperature; drug molecules were encapsulated into the NIRF nanogel by passive diffusion, and unloaded drugs were removed by extensive dialysis.[47] The drug-loading ability of the NIRF nanogel could be attributed to an intermolecular force such as the van der Waals force between the two. DLC and DLE of the NIRF nanogel were calculated to be 11.2% and 70%, respectively. Drug release behavior of the doxorubicin-loaded NIRF nanogel was studied under both reduction-insensitive and reduction-sensitive conditions, and the results are shown in Figure 4. Under reduction-insensitive conditions, the cumulative amount of drug released from the NIRF nanogel reaches 68% after incubating at PBS for 10 h, with no more drug released afterward, while under reduction-sensitive conditions, a GSH-promoted drug release was observed, with a total release of the 88% drug after a period of 10 h. It is worth noticing that drug release under reduction-insensitive conditions was also evident after 10 h of incubation in PBS. This may have resulted from the drug loading method employed: since the NIRF prodrug was cross-linked, diffusion of the drug into its dense core is slow and the loaded drug molecules mainly located at the outer part of the cross-linked core. Therefore, drug release was evident even under reduction-insensitive conditions. Stirring the solution at elevated temperature may facilitate the diffusion into the inner core, but when we performed the drug-loading experiment at 50 °C, the interaction between the dye and the drug molecules was pronounced, leading to the formation of NIRF prodrug with only very weak fluorescence; this may indicate the destruction of dye under these conditions.

In vitro toxicity of both the NIRF nanogel and NIRF prodrug were evaluated by a MTT method. Figure 5 shows the cell viability after incubating HeLa cells with NIRF nanogel and NIRF prodrug for 72 h at various concentrations. For NIRF nanogel, low toxicity could be observed up to a concentration of 0.1 mg/mL. Compared with NIRF nanogel, the toxicity of NIRF prodrug is significantly higher, even at low nanogel concentration (0.025 mg/mL), which could be attributed to the loaded doxorubicin.

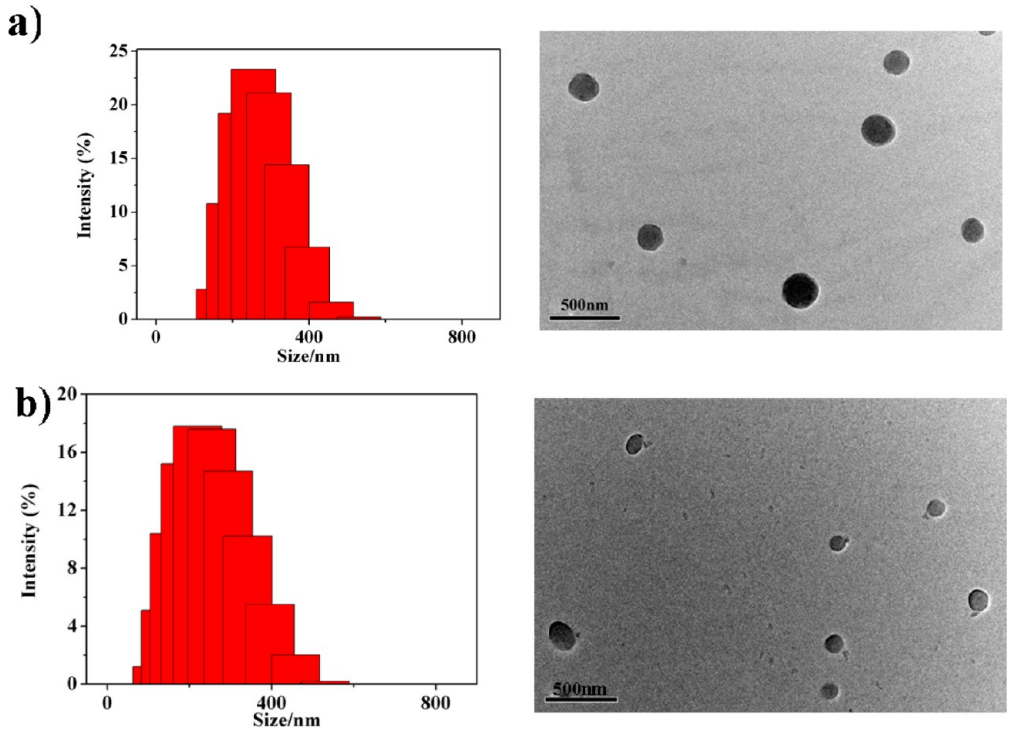

Figure 3. Size distribution and TEM image of (a) the parent nanogel and (b) the NIRF nanogel. DLS measurement was carried out at a nanogel concentration of 1 mg/mL, the nanogel solution has passed a 450-nm membrane just prior to measurement.

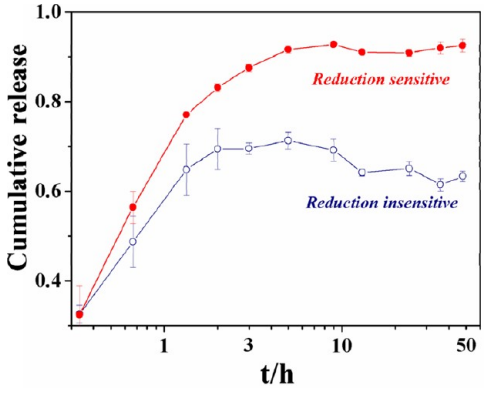

Figure 4. Drug release behavior of the NIRF nanogel under both reduction-sensitive and reduction-sensitive conditions.

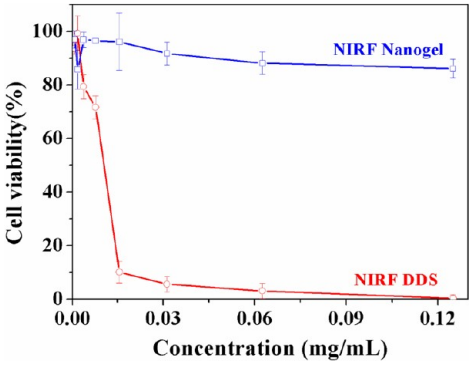

Figure 5. Cell viability of HeLa cells incubated with the NIRF nanogel and NIRF prodrug for 72 h.

To analyze the free aminocyanine, the NIRF nanogel, and the NIRF prodrug internalization and subcellular localization, we incubated the respective materials with cultured A549 cells and subsequently observed the cells under a laser confocal scanning microscope after 1, 4, and 8 h of culture. We labeled the cytoskeleton F-actin using Alexa 488-phalloidin and stained cell nuclei with DAPI. As shown in Figure 6, after 1 h incubation the fluorescence signal from aminocyanine moiety was detected in the cytoplasm for NIRF nanogel (Figure 6b) and NIRF prodrug (Figure 6c), and the fluorescence signal became stronger and dispersed in the cytoplasm as time went by (at 4 or 8 h), while only weak fluorescence signal could be detected for free aminocyanine (Figure 6a), demonstrating a much easier cell internalization of NIRF nanogel and NIRF prodrug than free aminocyanine by A549 cells. For NIRF prodrug (Figure 6c), signal corresponding to doxorubicin and aminocyanine were observed within the cytoplasm at 1 h, which may correspond to the release of doxorubicin from the NIRF prodrug in the presence of GSH. Figure 6d is the enlarged image of Figure 6c, and it clearly shows that the signals of doxorubicin and cyanine-conjugated polymer were separated efficiently after 8 h and may correspond to the disassembly of the NIRF nanogel under the reduction-sensitive conditions in cytoplasm and subsequent release of the drug.

Tumor localization ability of both the NIRF nanogel and NIRF prodrug were investigated by a whole body imaging method on nude mice. Fluorescence signal of the materials was recorded as a function of time, and the results are shown in Figure 7a. As time went by, the two materials show similar in vivo behavior and gradually accumulated at tumor and liver place (48 h). Tumor site accumulation could be attributed to the highly permeable vascular structure of the neoplasm, which always leads to a passive accumulation of nanosized materials (EPR effect[49]), while liver site accumulation occurred because liver is the major organ that uptakes and accumulates any types of nano/micro particles.[50] Ex vivo imaging was also performed

dx.doi.org/10.1021/am301600u | ACS Appl. Mater. Interfaces 2012, 4, 5662−5672

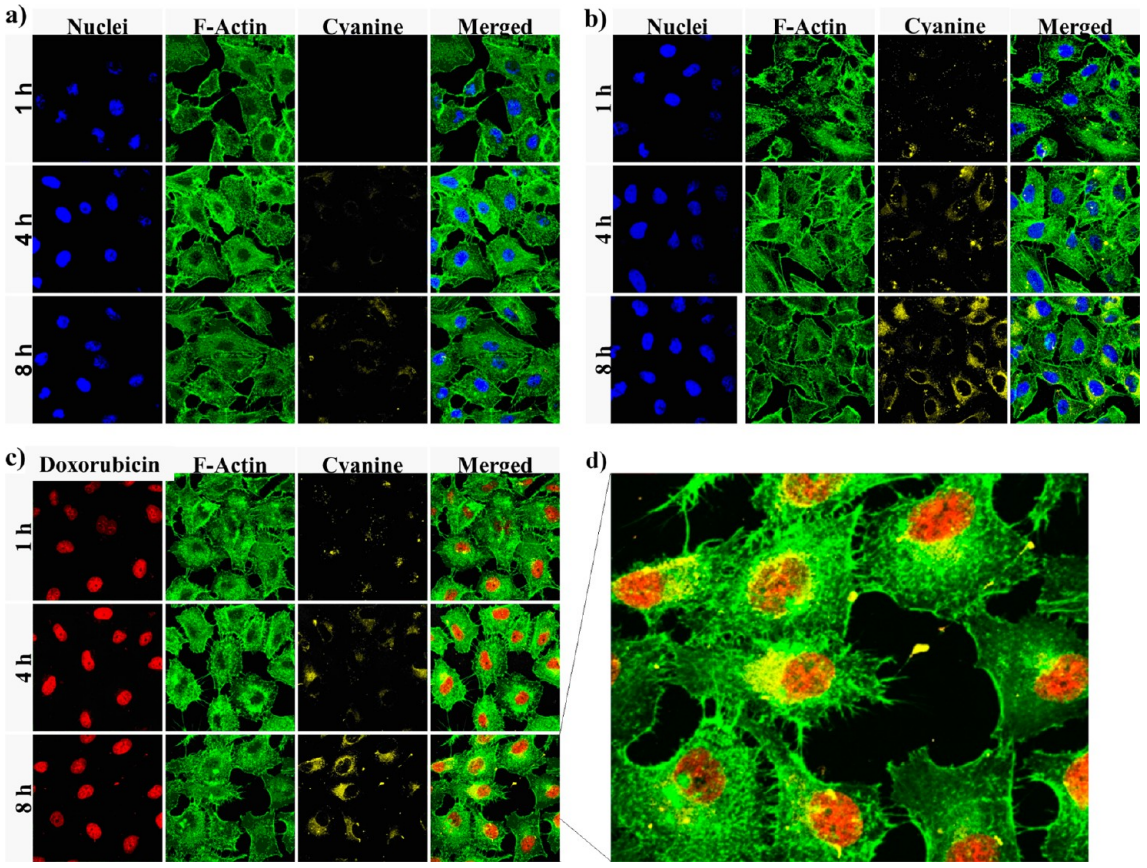

Figure 6. In vitro cellular uptake studies of (a) free aminocyanine, (b) NIRF nanogel, and (c) NIRF prodrug at 1, 4, and 8 h. Panel d is an enlarged image of the merged image in panel c. Legend: nuclei, stain blue with DAPI; green fluorescence, F-actin; red fluorescence, doxorubicin; yellow fluorescence, aminocyanine.

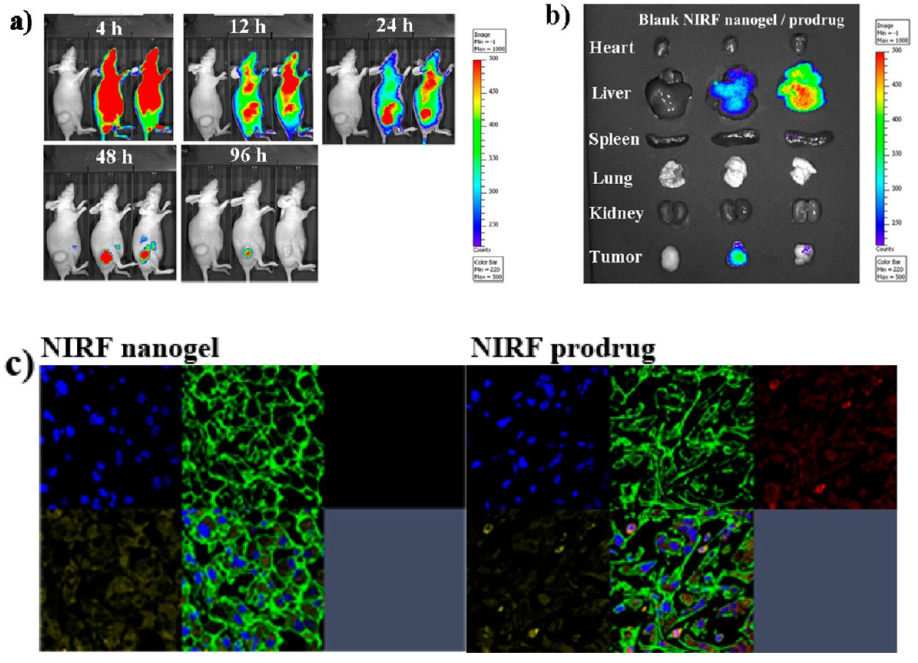

Figure 7. (a) In vivo NIRF imaging in A549 tumor-bearing mice after intravenous injection of the NIRF nanogel (middle) and NIRF prodrug (right) at different time points. Mouse without injection was used as reference (left). (b) Ex vivo NIRF imaging of major organs and tumor 96 h after injection of the NIRF nanogel and NIRF prodrug. (c) Confocal laser scanning microscopic of tumor slices (NIRF nanogel and NIRF prodrug refer to tumor excised from mouse injected with NIRF nanogel and NIRF prodrug). Legend: nuclei, stain blue with DAPI; green fluorescence, F-actin; red fluorescence, doxorubicin; yellow fluorescence, aminocyanine.

to study biodistribution of the two materials. Mice were sacrificed at 96 h after injection, and the fluorescence intensity of obtained organs and tumor were examined. As shown in Figure 7b, fluorescence signal from liver and tumor could also be detected after 96 h of injection. Long fluorescence time of the materials may be attributed to the pegylation nature of the nanogel, which is usually assumed to improve the system stability against serum during blood circulation. It is interesting to note that the NIRF nanogel and NIRF prodrug show different accumulation behavior in vivo. In Figures 7a and 7b, both the NIRF nanogel and NIRF prodrug accumulated at liver and tumor places after 12 h; the NIRF nanogel mainly accumulated at the tumor after 24 h, while a substantial amount of NIRF prodrug still remained at the liver place after the same time. Ex vivo NIRF imaging after 96 h (Figure 7b) also shows that liver is the major organ where NIRF prodrug accumulated, the difference between the two materials may be due to the size difference of the two nanoparticles. After loading of doxorubicin, the average diameter of the nanoparticle determined by DLS increase from 232 nm to 300 nm (data not shown). NIRF prodrug of larger size is much more prone to uptake by reticuloendothelial system (RES) organs such as liver, as reported in the literature;[51−53] thus, a much more pronounced liver accumulation of this material was observed. To investigate whether the two materials could enter tumor cell via endocytosis, excised tumor was sliced and the fluorescence of the obtained slice was examined; the results are shown in Figure 7c. Clearly, both the NIRF nanogel and the NIRF prodrug could enter the cell and become finely distributed in the cytoplasm. For the NIRF prodrug, drug signal from cytoplasm could also be detected, indicating that the drug has been successfully transported into the tumor cell.

CONCLUSIONS

A reduction-sensitive polypeptide nanogel conjugated with a near-infrared fluorescence (NIRF) cyanine probe has been synthesized. The anticancer drug doxorubicin was then loaded into the obtained NIRF nanogel via physical encapsulation. In vitro drug release experiment of the NIRF prodrug shows reduction-promoted drug release behavior in the presence of GSH. In vivo circulation behavior of both the NIRF nanogel and NIRF prodrug were also studied by a whole body imaging method on nude mice; the results show that both of the two materials could localize tumor tissue via EPR mechanism. The NIRF prodrug synthesized here has the potential application for the theranosis of cancer.

EXPERIMENTAL SECTION

Materials. All the chemicals had analytical-reagent (AR) purity, except those specifically indicated, and were purchased from Sinoreagent Corporation. Dichloromethane (DCM) and THF were first refluxed with CaH_2 followed by distillation. *N*,*N*-Dimethylformamide (DMF) was dried over CaH_2 at room temperature for 24 h before vacuum distillation. Glutathione (reduced form), diisopropylethylamine (DIEA), 2,3,3-trimethylbenzoindolenine, 3-bromopropionic acid, triphosgene, doxorubicin hydrochloride, and nepsilon-carbobenzoxy-L-lysine were purchased from Aladdin Corporation (China). A dialysis bag (cutoff M_w = 8000) was obtained from Bomei Biotechnology Corporation (China). mPEG (M_w =1900) were purchased from Aldrich and used as-received, without further purification. Milli-Q water (18.2 MΩ) was prepared using a Milli-Q Synthesis System (Millipore, Bedford, MA, USA). Column chromatography was performed using 200−300 mesh silica gel (Yantai Institute of Chemical Engineering, China).

Characterization. ^{1}H NMR spectra were either measured on a Bruker AC 300 or Bruker AC 400 spectrometer, as indicated. Deuterated dimethyl sulfoxide (DMSO) containing 0.03% (v/v) tetramethylsilane (TMS) was used as the solvent. FT-IR spectra were measured on a Bruker EQUINOX 55 Fourier transform infrared (FT-IR) spectrometer using the KBr disk method, and the liquid sample was coated onto a KBr disk before analysis. Transmission electron microscopy (TEM) measurement was performed on a JEOL-2010 microscope with an accelerating voltage of 200 KV. Size and size distribution of the nanogel were determined by dynamic light scattering (DLS) carried out on a Malvern Zetasizer Nano ZS90 with a He−Ne laser (633 nm) and 90° collecting optics. Measurements were performed at room temperature, and the data were analyzed by Malvern Dispersion Technology Software 4.20. Fluorescence measurements were carried out on a Shimadzu Model RF-5301PC fluorescence spectrophotometer with an excitation and emission slit width of 5 and 15 nm, respectively. UV−vis spectra were obtained on a Shimadzu Model UV-2401PC ultraviolet spectrophotometer. ESI mass spectra were obtained on a LCQ Advantage MAX Spectrometer, using methanol solutions of the sample.

The molar extinction coefficient (ε) of the sample was determined by Beer's law, based on three separate measurements. The relative fluorescence quantum yield (Φ_F) was determined using the following equation:[54]

$$\Phi_{F(x)} = \left(\frac{A_s}{A_x}\right)\left(\frac{F_x}{F_s}\right)\left(\frac{n_x}{n_s}\right)^2 \Phi_{F(s)}$$

where Φ, A, and n refer to the quantum yield, absorption, and refractive index of the solvents used. F_x stands for the area under emission curve. The subscripts x and s represent the sample value and the standard value, respectively. Indocyanine green (ICG) was used as a reference with a quantum yield of 0.078 in MeOH.[55]

Synthesis of 1-Hydroxycarbonylethyl-2,3,3-trimethylbenzoindoleninium Bromide (1).[35] 2,3,3-Trimethylbenzoindolenine (4.0 g, 19.1 mmmol) was dissolved in 30 mL of 1,2-dichlorobenzene, followed by the addition of 3-bromopropionic acid (2.9 g, 19.1 mmol), the obtained mixture was refluxed at 85 °C for 10 h. On cooling the solution after reaction, product 1 separated from the solution as gray solids. The obtained gray solids were washed with a mixture of ether and chloroform, dried under vacuum, and used without further purification.

Yield = 75%. ^{1}H NMR (300 MHz, DMSO) δ: 8.37 (d, J = 8.4 Hz, 1H), 8.28 (d, J = 9.0 Hz, 1H), 8.19 (dd, J = 16.6, 8.4 Hz, 1H), 7.76 (dt, J = 15.3, 6.9 Hz, 2H), 4.77 (t, J = 7.0 Hz, 2H), 3.04 (t, J = 7.0 Hz, 2H), 2.96 (s, 3H), 1.75 (s, 6H). MS (m/z, ESI): calcd for $C_{18}H_{20}NO_2$, 282.2; found: 282.1 [M−Br$^-$]$^+$.

Synthesis of 2-Chloro-1-formyl-3-(hydroxymethylene)cyclohex-1-ene (2). To an ice-cooled solution of DMF (40 mL, 520 mmol) in DCM, a solution of $POCl_3$ (37 mL, 397 mmol) in DCM (35 mL) was slowly added via an addition funnel. After the addition was completed, cyclohexanone (10 g, 100 mmol) was added via a syringe. The obtained solution was heated to reflux for 2 h. The oil-like red

residue was then poured into 100 mL of ice. The resultant mixture was kept at 4 °C overnight to allow the bisaldehyde (**2**) to crystallize. The yellow crystals were filtered off the solution, followed by crystallization from a mixture of acetone and DCM twice to give the bisaldehyde **2** as a yellow solid (7.8 g, 45% yield).

^{1}H NMR (400 MHz, DMSO) δ: 10.82 (s, 1H), 2.33 (overlap with solvent signal, 4H), 1.80−1.43 (m, 2H). MS (*m*/*z*, ESI): calcd for $C_8H_8ClO_2$, 171.0; found, 171.0 $[M-H^+]^-$.

Synthesis of Parent Cyanine Dye (3). Quatemary ammonium salt 1 (0.42 g, 1.16 mmol) and bisaldehyde **2** (0.10 g, 0.58 mmol) were dissolved into a mixture solvent of benzene (15 mL) and *n*-butanol (35 mL) in a two-necked flask fitted with a Dean−Stark trap and a condenser. The mixture was heated to 110 °C under a nitrogen atmosphere for 16 h, after which the solvent was removed under vacuum. The obtained green solid was washed with ether and purified via normal-phase column chromatography with a gradient elution from EtOAc to EtOAc/methnol (5:1). Removing solvent after column chromatography yields 0.35 g of dye 3 (68% yield) as a deep green solid.

^{1}H NMR (300 MHz, DMSO, δ, ppm): 8.34 (dd, J = 22.4, 11.1 Hz, 4H), 8.09 (t, J = 8.2 Hz, 4H), 7.77 (d, J = 8.7 Hz, 2H), 7.58 (ddd, J = 23.5, 15.4, 7.8 Hz, 4H), 6.40 (t, J = 20.7 Hz, 2H), 4.63 (s, 4H), 3.96 (t, J = 6.1 Hz, 4H), 2.84 (d, J = 38.6 Hz, 8H), 1.95 (s, 16H), 1.57−1.32 (m, 4H), 1.20 (dd, J = 14.2, 6.9 Hz, 4H), 0.76 (t, J = 7.1 Hz, 6H). MS (*m*/*z*, ESI): calcd for $C_{52}H_{60}ClN_2O_4$, 811.3; found, 811.4 $[M-Br^-]^+$. ε = 183333 M^{-1} cm^{-1}, Φ_F = 0.082. R_f = 0.75 (MeOH:EtOAc = 1:6).

Synthesis of Aminocyanine Dye (4). Cyanine dye (**3**) (150 mg, 0.17 mmol) and 6-aminocaproic acid (30 mg, 0.23 mmol) was added to 5 mL of dry DMF, followed by the addition of 29 μL of DIEA (22 mg, 0.17 mmol). The obtained solution was heated to 70 °C and stirred at this temperature in darkness for 8 h. The solvent was then removed under vacuum, and the obtained deep blue solid was washed with ether and further purified by a column chromatography method with gradient elution from EtOAc to EtOAc/methanol (5:1). One hundred milligrams (100 mg) (59% yield) of deep blue solid were obtained after removing solvent under vacuum.

^{1}H NMR (300 MHz, DMSO, δ, ppm) 8.13 (t, J = 13.0 Hz, 2H), 7.96 (dd, J = 8.8, 6.1 Hz, 4H), 7.70 (d, J = 12.1 Hz, 2H), 7.56 (dd, J = 17.2, 8.5 Hz, 4H), 7.38 (dd, J = 16.3, 9.1 Hz, 2H), 5.84 (d, J = 12.9 Hz, 2H), 4.37 (s, 4H), 3.94 (t, J = 6.6 Hz, 4H), 3.76 (s, 2H), 2.78 (t, J = 6.9 Hz, 4H), 2.56 (4H, overlap with the solvent signal), 2.27 (t, J = 7.2 Hz, 2H), 1.95−1.71 (m, 18H), 1.70−1.55 (m, 2H), 1.47−1.36 (m, 4H), 1.26−1.14 (m, 4H), 0.94−0.83 (m, 2H), 0.76 (q, J = 7.3 Hz, 6H). MS (*m*/*z*, ESI): calcd for $C_{58}H_{72}N_3O_6$, 906.4; found, 906.5 $[M-Br^-]^+$. ε = 60000 M^{-1} cm^{-1}, Φ_F = 0.64. R_f = 0.83 (MeOH:EtOAc = 1:6).

Synthesis of Aminocyanine-OSu (5). Aminocyanine dye 4 (5.0 mg, 5.1 μmol) was dissolved into 1 mL of dry DMF solution, followed by the addition 1 mL DMF solution containing 0.69 mg HOSu (5.6 μmol) and 1.5 mg DCC (7.3 μmol). The obtained mixture was stirred in darkness for 24 h at room temperature, the above solution containing activated aminocyanine was directly used for the parent nanogel labeling without purification.

Synthesis of L-Cystine-NCA (6). This material was prepared according to our previous method.[46] Namely, (Z-Cys-OH)$_2$[56] (3.0 g, 5.9 mmol) was suspended in 50 mL dry DCM in an ice-cooled bath, 0.6 mL of PBr_3 (6.3 mmol) was added into it. The mixture was stirred at this temperature for 10 h, then warmed to room temperature and stirred overnight. The obtained white solid was washed repeatedly with dry DCM and dried on a vacuum line (1.48 g, 86% yield).

^{1}H NMR (400 MHz, DMSO, δ, ppm): 4.78(t, 1H), 2.95(dd, 1H), 3.02(dd, 1H). ^{13}C NMR (400 MHz, DMSO, δ, ppm): 170.3, 151.6, 56.9, 54.8, 39.6. FT-IR (KBr, thin film, cm^{-1}): 1780, 1850.

Synthesis of LLys-NCA (7). LLys NCA was prepared following a standard triphosgene method.[57] Nepsilon-carbobenzoxy-L-lysine (2.0 g, 7.1 mmol) was suspended in 50 mL of dry THF, then a THF solution of triphosgene (2.1 g, 8.9 mmol) was added into it, and the combined solution was stirred at 45 °C for 2 h, the obtained clear solution was precipitated into dry hexane. Precipitates were collected, followed by crystallization three times from a mixture of THF and hexane to give the anhydride as white crystals (1.6 g, 75% yield).

^{1}H NMR (400 MHz, DMSO, δ, ppm): 7.30−7.36 (m, 5H), 5.01 (s, 2H), 4.40 (dd, 1H), 2.96 (m, 2H), 1.63−1.71 (m, 2H), 1.28−1.41 (m, 4H). ^{13}C NMR (400 MHz, DMSO, δ, ppm): δ 171.8, 156.1, 152.0, 137.3, 128.4, 127.8, 65.1, 57.0, 41.3, 31.1, 30.6, 28.7.

Synthesis of Parent Nanogel (8). For the ring-opening polymerization, L-cystine-NCA (0.45 g, 1.54 mmol) and LLys-NCA (0.48 g, 1.57 mmol) was dissolved into 5 mL of dry DMF in a flame-dried flask under argon, then a DMF (15 mL) solution containing mPEG-NH_2 (0.59 g, 0.31 mmol) was added. The combined mixture was first stirred at 0 °C for 3 days, then heated to 45 °C and stirred at this temperature for one day. The polymer solution then was precipitated into 100 mL of cold ether; the product that separated from the mixture was redissolved in DMF, the DMF solution was dialyzed against 1 L of water for 48 h, during which the water was changed every 12 h. Removing the water by freeze-drying gives 0.58 g (44% yield) of the parent nanogel **8**.

Synthesis of NIRF Nanogel (9). The parent nanogel **8** (50 mg, 0.12 mmol NH_2 group) was dissolved into 1 mL of DMF, a DMF solution (1 mL) containing 12 μmol aminocyanine-OSu was added dropwise under vigorous stirring. The mixture then was stirred at room temperature for 12 h in darkness. The solution after reaction was first precipitated into 10 mL of cold ether, and then the collected precipitates were redissolved in DMF, followed by dialysis against 250 mL of water for 24 h (the water was changed every 12 h). Forty milligrams (40 mg) (80% yield) of NIRF nanogel were obtained after the water was removed by freeze-drying. The NIRF nanogels with dye substitution degrees of 25% and 50% were prepared in a similar manner.

Preparation of NIRF Prodrug. Doxorubicin hydrochloride (2.0 mg, 3.4 mmol) and 12.5 mg NIRF nanogel were dissolved into 2 mL of DMF; the obtained solution was stirred overnight in darkness, followed by dialysis against 100 mL of water for 36 h to remove free drug, during which the water was changed every 12 h. The amount of unloaded drug was quantified by analyzing the dialysate using a fluorospectrophotometer at an emission wavelength of 557 nm with an excitation wavelength of 480 nm and a slit width of 5 nm. The amount of drug loaded was determined by subtracting the amount of unloaded drug with drug fed. Drug loading content (DLC) and drug loading efficiency (DLE) are determined by the following equations:

$$\text{DLC (wt \%)} = \left(\frac{\text{weight of loaded drug}}{\text{weight of nanogel}}\right) \times 100$$

$$\text{DLE (wt \%)} = \left(\frac{\text{weight of loaded drug}}{\text{weight of drug fed}}\right) \times 100\%$$

Drug loading content and loading efficiency were determined to be 11.2% and 70%, respectively.

In Vitro Drug Release. Drug release behavior of doxorubicin-loaded NIRF nanogel was studied under both reduction-sensitive and reduction-insensitive conditions. For the reduction-insensitive conditions, 0.4 mL of drug-loaded NIRF nanogel solution (1 mg/mL) was sealed into a dialysis bag and submerged into 50 mL of 0.2 M phosphate-buffered saline (PBS). Release experiment was conducted at 37 °C on a shaking bath. Sample (2 mL) was removed at predetermined time points for analysis, while 2 mL of fresh PBS was added subsequently. Drug released was quantified by using a fluorospectrophotometer at an emission wavelength of 557 nm with an excitation wavelength of 480 nm and a slit width of 5 nm. For the reduction-sensitive conditions, a similar method was employed, except 0.2 M PBS containing 10 mM GSH was used as release media.

Cytotoxicity. Cytotoxicity of both the NIRF nanogel and the NIRF prodrug were evaluated with a methyl tetrazolium (MTT) viability assay against HeLa cell. HeLa cells were seeded in a 96-well plate with a cell number of 5000 cells per well. A 1640 solution containing 10% fetal bovine serum (FBS) was used as the cell culture media. After incubating at 37 °C for 24 h under a 5% CO_2 atmosphere, the culture media was replaced with a series of nanogel solution (in 1640 media containing 10% FBS) ranging from 0 to 0.25 mg/mL. The cells then were incubated at 37 °C for 2 days, and the culture media were removed and 100 μL fresh 1640 (10% FBS) was added to each well, followed by the addition of 25 μL MTT stock solution (5 mg/mL). One hundred microliters (100 μL) of extraction buffer (20% SDS in 50% DMF, pH 4.7, prepared at 37 °C) was added to each well after an additional incubation of 2 h. The obtained solution were incubated overnight, the absorbance of the solution was measured at 490 nm using a Bio-Rad 680 microplate reader. The cell viability was normalized to HeLa cells cultured in complete culture medium.

Cellular Uptake Study. A549 cells (7×10^4 cells/well) were seeded on coverslips in 24-well plates and incubated for 24 h. The aminocyanine, NIRF nanogel, or NIRF prodrug was then added to a final concentration of 0.03 mg/mL and incubated with the cells for 1, 4, or 8 h. Free aminocyanine solution was prepared by dissolved 2 mg of aminocyanine to 0.1 mL of DMSO, followed by the addition of 2 mL of H_2O to obtain a solution with a final concentration of 0.9 mg/mL. NIRF nanogel and NIRF prodrug solution were prepared by first dissolving the material into DMSO, following by extensive dialysis against water. After removing the medium, cells were washed twice with cold phosphate buffered saline (PBS, pH 7.4, 0.01 M) and fixed with 4% formaldehyde (Sigma–Aldrich, St. Louis, MO, USA). To label the cytoskeleton, samples were incubated with Alexa Fluor 488-phalloidin (Invitrogen, Carlsbad, CA, USA) at 25 °C for 20 min (after incubation with 1 mg/mL bovine serum albumin (BSA) in PBS to decrease nonspecific interactions) followed by rinsing with PBS. To label the cell nucleus, samples were incubated with 1 mg/mL DAPI (Beyotime, Haimen, PRC) for 5 min in PBS, followed by extensive rinsing with PBS. Slides were mounted with one drop of Fluoromount aqueous mounting medium (Invitrogen) and observed using a Zeiss Model LSM 710 laser confocal scanning microscope imaging system (Heidenheim, Germany) with an upright confocal microscope and an excitation wavelength of 633 nm.

In Vivo Animal Study. Female athymic (nu/nu) mice were obtained from the Vital River Laboratory Animal Technology Co., Ltd. (Beijing, PRC), and used at 8 weeks of age. All animals received care in compliance with the guidelines outlined in the *Guide for the Care and Use of Laboratory Animals*, and all procedures were approved by the University of Science and Technology of China Animal Care and Use Committee.

A xenograft tumor model was generated by subcutaneous injection of A549 cells (3×10^6/100 μL) into the right flank of nude mice. For in vivo imaging, female mice bearing A549 tumors were administered 200 μL of the NIRF nanogel aqueous solution (1 mg/mL), or an equivalent amount of NIRF prodrug solution, or PBS by intraveneous injection. Animals were placed onto the warmed stage inside of an IVIS light-tight chamber and anesthesia was maintained with 2.5% isofluorane. Image acquisition was performed at different time intervals on a Xenogen IVIS Lumina system (Caliper Life Sciences, USA). Results were analyzed using Living Image 3.1 software (Caliper Life Sciences). At the end of the experiment, the mice were sacrificed, and major organs and tumor tissues were collected. For laser confocal scanning microscope analysis, the tissues were fixed in 4% paraformaldehyde overnight at 4 °C, and then immersed overnight in 30% sucrose solution. Tumor tissues were sectioned (7 μm thick). To label the cytoskeleton, samples were incubated with Alexa Fluor 488-phalloidin (Invitrogen) at 25 °C for 20 min, followed by counterstained with DAPI. Slides were mounted with one drop of Fluoromount aqueous mounting medium (Invitrogen) and observed using a Zeiss Model LSM 710 laser confocal scanning microscope imaging system (Heidenheim) with an upright confocal microscope and excitation wavelength of 675 nm.

■ ASSOCIATED CONTENT

Supporting Information

Mass spectra of parent cyanine (**3**) and aminocyanine (**4**). This material is available free of charge via the Internet at http://pubs.acs.org.

■ AUTHOR INFORMATION

Corresponding Author

*Tel.: +86-551-3606853. Fax: +86-551-3603748. E-mail: lfyan@ustc.edu.cn.

Notes

The authors declare no competing financial interest.

■ ACKNOWLEDGMENTS

Professor Jun Wang of USTC is greatly appreciated for both his beneficial discussion with us and his helpful suggestion with animal experiment. We would also like to thank the National Natural Science Foundation of China (Nos. 20874095 and 50173147) for the financial support.

■ REFERENCES

(1) Lian, T.; Ho, R. J. Y. *J. Pharm. Sci.* **2001**, *90*, 667–680.

(2) Kratz, F.; Beyer, U.; Schutte, M. T. *Crit. Rev. Ther. Drug Carrier Syst.* **1999**, *16*, 245−288.
(3) Rodrigues, P. C. A.; Beyer, U.; Schumacher, P.; Roth, T.; Fiebig, H. H.; Unger, C.; Messori, L.; Orioli, P.; Paper, D. H.; Mulhaupt, R.; Kratz, F. *Biorg. Med. Chem.* **1999**, *7*, 2517−2524.
(4) Duncan, R. *Nat. Rev. Drug Discovery* **2003**, *2*, 347−360.
(5) Kataoka, K.; Harada, A.; Nagasaki, Y. *Adv. Drug Delivery Rev.* **2001**, *47*, 113−131.
(6) Kataoka, K.; Kwon, G. S.; Yokoyama, M.; Okano, T.; Sakurai, Y. *J. Controlled Release* **1993**, *24*, 119−132.
(7) Torchilin, V. P. *J. Controlled Release* **2001**, *73*, 137−172.
(8) Lin, W.; Kim, D. *Langmuir* **2011**, *27*, 12090−12097.
(9) Zhang, L.; Liu, W.; Lin, L.; Chen, D.; Stenze, M. H. *Biomacromolecules* **2008**, *9*, 3321−3331.
(10) Ryu, J.-H.; Chacko, R. T.; Jiwpanich, S.; Bickerton, S.; Babu, R. P.; Thayumanavan, S. *J. Am. Chem. Soc.* **2010**, *132*, 17227−17235.
(11) Aulenta, F.; Hayes, W.; Rannard, S. *Eur. Polym. J.* **2003**, *39*, 1741−1771.
(12) Kolhe, P.; Misra, E.; Kannan, R. M.; Kannan, S.; Lieh-Lai, M. *Int. J. Pharm.* **2003**, *259*, 143−160.
(13) Lee, C. C.; MacKay, J. A.; Frechet, J. M. J.; Szoka, F. C. *Nat. Biotechnol.* **2005**, *23*, 1517−1526.
(14) Gil, E. S.; Hudson, S. M. *Prog. Polym. Sci.* **2004**, *29*, 1173−1222.
(15) Gillies, E. R.; Frechet, J. M. J. *Bioconjugate Chem.* **2005**, *16*, 361−368.
(16) Tang, L.-Y.; Wang, Y.-C.; Li, Y.; Du, J.-Z.; Wang, J. *Bioconjugate Chem.* **2009**, *20*, 1095−1099.
(17) Meng, F.; Hennink, W. E.; Zhong, Z. *Biomaterials* **2009**, *30*, 2180−2198.
(18) Wu, G. Y.; Fang, Y. Z.; Yang, S.; Lupton, J. R.; Turner, N. D. *J. Nutr.* **2004**, *134*, 489−492.
(19) Kim, K. S.; Hur, W.; Park, S.-J.; Hong, S. W.; Choi, J. E.; Goh, E. J.; Yoon, S. K.; Hahn, S. K. *ACS Nano* **2010**, *4*, 3005−3014.
(20) Bagalkot, V.; Zhang, L.; Levy-Nissenbaum, E.; Jon, S.; Kantoff, P. W.; Langer, R.; Farokhzad, O. C. *Nano Lett.* **2007**, *7*, 3065−3070.
(21) Erathodiyil, N.; Ying, J. Y. *Acc. Chem. Res.* **2011**, *44*, 925−935.
(22) Peng, C.-L.; Shih, Y.-H.; Lee, P.-C.; Hsieh, T. M.-H.; Luo, T.-Y.; Shieh, M.-J. *ACS Nano* **2011**, *5*, 5594−5607.
(23) Sun, C.; Pratx, G.; Carpenter, C. M.; Liu, H.; Cheng, Z.; Gambhir, S. S.; Xing, L. *Adv. Mater.* **2011**, *23*, H195−H199.
(24) Altinoglu, E. I.; Russin, T. J.; Kaiser, J. M.; Barth, B. M.; Eklund, P. C.; Kester, M.; Adair, J. H. *ACS Nano* **2008**, *2*, 2075−2084.
(25) Xiong, X. B.; Lavasanifar, A. *ACS Nano* **2011**, *5*, 5202−5213.
(26) Masotti, A.; Vicennati, P.; Boschi, F.; Calderan, L.; Sbarbati, A.; Ortaggi, G. *Bioconjugate Chem.* **2008**, *19*, 983−987.
(27) Cho, H.-J.; Yoon, I.-S.; Yoon, H. Y.; Koo, H.; Jin, Y.-J.; Ko, S.-H.; Shim, J.-S.; Kim, K.; Kwon, I. C.; Kim, D.-D. *Biomaterials* **2012**, *33*, 1190−200.
(28) Weissleder, R.; Ntziachristos, V. *Nat. Med.* **2003**, *9*, 123−128.
(29) Narayanan, N.; Patonay, G. *J. Org. Chem.* **1995**, *60*, 2391−2395.
(30) Peng, X. J.; Song, F. L.; Lu, E.; Wang, Y. N.; Zhou, W.; Fan, J. L.; Gao, Y. L. *J. Am. Chem. Soc.* **2005**, *127*, 4170−4171.
(31) Bae, Y.; Kataoka, K. *Adv. Drug Delivery Rev.* **2009**, *61*, 768−784.
(32) Hadjichristidis, N.; Iatrou, H.; Pitsikalis, M.; Sakellariou, G. *Chem. Rev.* **2009**, *109*, 5528−5578.
(33) Choi, Y. H.; Liu, F.; Kim, J. S.; Choi, Y. K.; Park, J. S.; Kim, S. W. *J. Controlled Release* **1998**, *54*, 39−48.
(34) Miyata, K.; Oba, M.; Nakanishi, M.; Fukushima, S.; Yamasaki, Y.; Koyama, H.; Nishiyama, N.; Kataoka, K. *J. Am. Chem. Soc.* **2008**, *130*, 16287−16294.
(35) Zhang, Z. R.; Achilefu, S. *Org. Lett.* **2004**, *6*, 2067−2070.
(36) Klok, H. A.; Rodriguez-Hernandez, J. *Macromolecules* **2002**, *35*, 8718−8723.
(37) Peng, S.-M.; Chen, Y.; Hua, C.; Dong, C.-M. *Macromolecules* **2009**, *42*, 104−113.
(38) Choi, Y. R.; Bae, Y. H.; Kim, S. W. *Macromolecules* **1998**, *31*, 8766−8774.
(39) Deming, T. J. *Adv. Mater.* **1997**, *9*, 299−311.
(40) Sulistio, A.; Lowenthal, J.; Blencowe, A.; Bongiovanni, M. N.; Ong, L.; Gras, S. L.; Zhang, X.; Qiao, G. G. *Biomacromolecules* **2011**, *12*, 3469−3477.
(41) Gao, H. F.; Tsarevsky, N. V.; Matyjaszewski, K. *Macromolecules* **2005**, *38*, 5995−6004.
(42) Ornelas, C.; Lodescar, R.; Durandin, A.; Canary, J. W.; Pennell, R.; Liebes, L. F.; Weck, M. *Chem.—Eur. J.* **2011**, *17*, 3619−3629.
(43) Kele, P.; Li, X.; Link, M.; Nagy, K.; Herner, A.; Lorincz, K.; Beni, S.; Wolfbeis, O. S. *Org. Biomol. Chem.* **2009**, *7*, 3486−3490.
(44) Ornelas, C.; Pennell, R.; Liebes, L. F.; Weck, M. *Org. Lett.* **2011**, *13*, 976−979.
(45) Ko-Jie, C.; Ya-Ling, C.; Yu-Ming, C.; Yi-Cheng, H.; Hsing-Wen, S. *Biomaterials* **2011**, *32*, 2586−2592.
(46) Xing, T.; Lai, B.; Ye, X.; Yan, L. *Macromol. Biosci.* **2011**, *11*, 962−969.
(47) Xiong, M.-H.; Wu, J.; Wang, Y.-C.; Li, L.-S.; Liu, X.-B.; Zhang, G.-Z.; Yan, L.-F.; Wang, J. *Macromolecules* **2009**, *42*, 893−896.
(48) Mishra, A.; Behera, R. K.; Behera, P. K.; Mishra, B. K.; Behera, G. B. *Chem. Rev.* **2000**, *100*, 1973−2011.
(49) Matsumura, Y.; Maeda, H. *Cancer Res.* **1986**, *46*, 6387−6392.
(50) Kim, J.-Y.; Il Choi, W.; Kim, Y. H.; Tae, G. *J. Controlled Release* **2011**, *156*, 398−405.
(51) Li, S.-D.; Huang, L. *Mol. Pharmaceutics* **2008**, *5*, 496−504.
(52) Qin, W.; Ding, D.; Liu, J.; Yuan, W. Z.; Hu, Y.; Liu, B.; Tang, B. Z. *Adv. Funct. Mater.* **2012**, *22*, 771−779.
(53) Zhang, L.; Yang, M.; Wang, Q.; Li, Y.; Guo, R.; Jiang, X.; Yang, C.; Liu, B. *J. Controlled Release* **2007**, *119*, 153−162.
(54) Demas, J. N.; Crosby, G. A. *J. Am. Chem. Soc.* **1971**, *93*, 2841−2847.
(55) Benson, R. C.; Kues, H. A. *Phys. Med. Biol.* **1978**, *23*, 159−163.
(56) Bischoff, L.; David, C.; Roques, B. P.; Fournie-Zaluski, M. C. *J. Org. Chem.* **1999**, *64*, 1420−1423.
(57) Daly, W. H.; Poche, D. *Tetrahedron Lett.* **1988**, *29*, 5859−5862.